Reactivity Descriptors and Rate Constants for Acid Zeolite Catalyzed Ethylation and Isopropylation of Benzene

Ann M. Vos,[†] Robert A. Schoonheydt,*[†] Frank De Proft,[‡] and Paul Geerlings[‡]

Center for Surface Chemistry and Catalysis, Katholieke Universiteit Leuven, Kasteelpark Arenberg 23, 3001 Leuven, Belgium, and Eenheid Algemene Chemie, Vrije Universiteit Brussel, Pleinlaan 2, 1050 Brussel, Belgium

Received: June 24, 2002; In Final Form: October 4, 2002

The acid zeolite catalyzed ethylation and isopropylation of benzene with ethene and propene is investigated at the B3LYP/6-31G* level of calculation with a T_4-cluster representing the Brønsted acid site of the zeolite. After geometry optimization of reactants, transition structures, and products, a kinetic and a sensitivity analysis were used to model the reactions. These reactions proceed in one step, without formation of alkoxy species or charged intermediates. Both reaction rate constants and local HSAB properties indicate that isopropylation is favored over ethylation, in agreement with experimental observations.

1. Introduction

Ethylbenzene and cumene are produced in large quantities in the petrochemical industry, as they are the starting materials for the production of styrene and phenol, respectively.[1] Ethylbenzene and cumene are primarily produced by benzene alkylation with ethene and propene, and the conventional catalysts are $AlCl_3$ or supported H_3PO_4. Unfortunately, these commercial processes present serious ecological problems such as corrosion and the disposal of spent harmful catalysts. To circumvent these problems, new technologies were introduced the past two decades for instance by Dow Chemical−Kellog and Mobil−Badger.[1] Here, acid zeolite based catalysts are used in the alkylation of benzene, and they offer the additional advantage to suppress formation of undesired diisopropylbenzenes, *n*-propylbenzenes, and chlorinated products. Experimentally, these reactions are studied extensively.[2]

Most theoretical studies of these reactions focus on the diffusion and adsorption of reaction products in the zeolite channels and are based on molecular dynamic methods.[3] Quantum mechanical methods enable the theoretical study of the mechanism of reactions catalyzed by Brønsted acid zeolites.[4] However, for the ethylation and isopropylation of benzene, these quantum mechanical methods have not yet been used much.

Sponer et al.[5] investigated the steric effect imposed by the channels of zeolites on the iso-/*n*-propylbenzene ratio. The molecules, protonated isopropylbenzene and benzene, were optimized using an HF/6-31G** level of theory. Only in the presence of steric constraints, similar to MFI and MEL zeolite channels, there exists a reaction pathway leading to *n*-propylbenzene, in agreement with the experimental observation.

Deka et al.[6] demonstrated that, besides shape selectivity, electronic factors play a subtle role in controlling selectivity. The influence of the zeolite composition on the ortho/para selectivity in the production of *para*-isobutylethylbenzene can be identified after calculation of the local softness.

Song et al.[7] used PM3 calculations to show that steric constraints imposed by the channels of mordenite have an effect on the frontier electron density of 2-isopropylnaphthalene thus inducing selectivity for 2,6-diisopropylnaphthalene, in agreement with the experimental observation.

Clark et al.[8] calculated the overlap between Fukui functions of the aromatic and the electrophilic alkyl group as a measure for the tendency for electrons to transfer from the aromatic to the alkyl group and therefore as a measure for the probability of reaction. When these quantum mechanical calculations are combined with molecular mechanics methods, a para selectivity in the methylation, ethylation, and isopropylation reaction of toluene using mordenite as catalysts is found.

When using quantum mechanics to model reactions catalyzed by acid zeolites, a cluster is often used to represent the active site of zeolites.[4a−d] This cluster is a small part cut out of the zeolite lattice. It contains a Brønsted acid site and some atoms around that site, and it is terminated with hydrogen atoms at the dangling bonds to preserve electrostatic neutrality. Although influence of the complete zeolite lattice is ignored, it has been proven possible to describe qualitatively the course of acid zeolite catalyzed reactions, using cluster approximations.[4a−d] The zeolite lattice can have an effect on (1) the geometry of adsorbed molecules and transition structures, due to, among others, steric constraints, and (2) the relative energy differences between the different structures. Because cluster models do not generate steric constraints on the geometry, they can be applied to model reactions catalyzed by large pore zeolites, like faujasite. The relative energy differences between the different structures can be influenced by the electrostatic effect of the zeolite lattice. It has been shown that charged species, e.g., transition structures, are stabilized by the zeolite framework while neutral species are less affected. Consequently, the calculated activation energies can decrease by 10−50% when the zeolite lattice is taken into account by full structure calculations.[9]

In this work, density functional calculations were done to find all structures involved in the ethylation and isopropylation of benzene (see Figure 1). A T_4 cluster was used to represent the zeolite acid site. This cluster offers the possibility to calculate reaction rate constants and reactivity descriptors.[10]

* To whom correspondence should be addressed. Fax: +32 16 321998. E-mail: robert.schoonheydt@agr.kuleuven.ac.be.
[†] Katholieke Universiteit Leuven.
[‡] Vrije Universiteit Brussel.

10.1021/jp026368v CCC: $25.00
Published on Web 02/06/2003

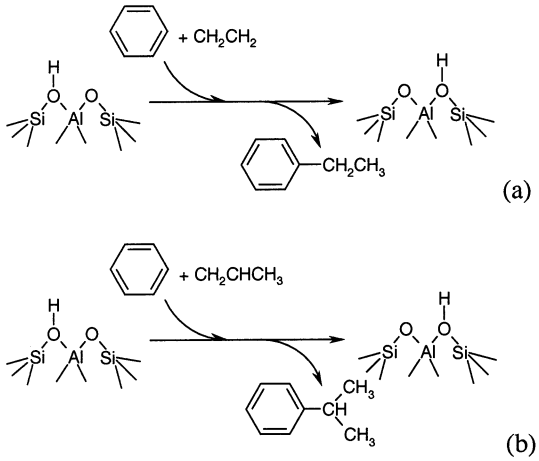

Figure 1. Studied reactions: (a) ethylation of benzene and (b) isopropylation of benzene.

2. Method

2.1. Geometry Optimization. All reactants, transition structures, and products are localized with cluster type calculations. During the geometry optimization, we look for a local minimum for reactants and products and for a first order saddle point for transition structures. On the stationary points, frequencies are evaluated analytically to check whether the obtained structures have the correct number of imaginary frequencies: none for minima and one for transition structures. The cluster we used consists of four T atoms (one Al and three Si) and was allowed to relax completely during the optimizations. Full relaxation of the cluster is usually essential for finding real stationary points during geometry optimizations. The size of the cluster can have an effect on quantitative properties such as proton affinities and OH stretching frequencies,[11] but for a qualitative description of acid zeolite catalyzed reactions, a T_4 cluster has been shown to be sufficient.[9a]

All calculations were done with Gaussian 98,[12] using the B3LYP functional[13] and a 6-31G* basis set. This level of calculation has been shown by Zygmunt et al.[14] to be a good choice for describing the course of acid zeolite catalyzed reactions.

2.2. Reaction Rate Constants. The reaction rate constants of the studied reactions are evaluated by using the canonical transition state theory of Eyring and co-workers.[15] A complete description of the method has been published before.[10] The reaction rate constant, k_r, for the reaction where two molecules *A* and *B* react simultaneously with a zeolite (*HZ*), is given by

$$k_r = (N_A V)^2 \left(\frac{k_B T}{h}\right) \frac{Q^{\ddagger}_{TS}}{Q_A\, Q_B\, Q_{HZ}}\, e^{-E_{bar}/RT} \qquad (1)$$

with N_A Avogadro's number, V the molar volume, k_B and h the constants of Boltzman and Planck constants, and T the temperature. E_{bar} is the activation barrier of the reaction. It is the energy difference between the reactants and the transition state containing already the zero point energy corrections. The partition functions Q_i and $Q^{\ddagger}_{TS}$ are evaluated using a rigid rotor harmonic oscillator approximation,[15] and we assumed that rotational (r), vibrational (v), and electronic (e) movements are independent of each other, $Q = Q_t Q_r Q_v Q_e$, where Q_t is the translational partition function. The molecular partition functions are obtained after a vibrational analysis by Gaussian 98, where the frequencies were scaled according to the procedure proposed by Scott et al.[16] With eq 1, we calculated the rate constants for a temperature ranging from 300 to 800 K. Reaction rate constants, calculated this way, seem to give a lower limit for zeolites with a high Si/Al ratio.[10a]

Kinetic data are often analyzed in terms of an Arrhenius expression[15a]

$$k_r = A e^{-E_{Arr}/RT}$$

$$\ln k_r = \ln A - \frac{E_{Arr}}{RT} \qquad (2)$$

where E_{Arr} is the Arrhenius activation energy and A the preexponential factor. When $\ln(k_r)$ is plotted against T^{-1}, a straight line is obtained with slope $-E_{Arr}\, R^{-1}$ and intercept $\ln(A)$. The preexponential factor, A, is proportional to the entropy difference between reactants and transition state, ΔS_{act}[15c]

$$\Delta S_{act} = R\left[\ln A - \ln\left(\frac{k_B T}{h}\right) - (1 - \Delta n) + \ln V^{\Delta n}\right] \qquad (3)$$

Δn being the change in the number of molecules from the reactants to the transition state.

2.3. Density Functional Based Reactivity Descriptors. Conceptual density functional theory[17] (DFT) provides a framework to discuss reactions in terms of changing number of electrons, N, and/or changing external potential, $v(r)$, (i.e., due to the nuclei). Within this conceptual branch of DFT the global hardness, η, is defined as the second derivative of the energy, E, with respect to the number of electrons, N[18]

$$\eta = \frac{1}{2}\left(\frac{\partial^2 E}{\partial N^2}\right)_{v(\mathbf{r})} = \frac{1}{2S} \qquad (4)$$

where S is the global softness. In the finite difference approach η can be written as

$$\eta = \frac{IE - EA}{2} \qquad (5)$$

with IE and EA the first vertical ionization energy and the electron affinity of the molecule. In the frozen core approximation, η equals the HOMO−LUMO gap

$$\eta = \frac{E_{LUMO} - E_{HOMO}}{2} \qquad (6)$$

The Fukui function, $f(r)$, is a mixed second-order derivative of the energy of the system with respect to N and the potential $v(\mathbf{r})$[19]

$$f(\mathbf{r}) = \left(\frac{\partial^2 E}{\partial N\, \partial v(\mathbf{r})}\right) \qquad (7)$$

The Fukui function is a reactivity index for orbital controlled reactions: the larger the value of the Fukui function, the higher the reactivity.[20] The condensed form of the Fukui function,[21] i.e., the Fukui function per atom k in a molecule using atomic populations, can be expressed as

$$f_k^{+} = [q_k(N+1) - q_k(N)] \qquad (8)$$

$$f_k^{-} = [q_k(N) - q_k(N-1)] \qquad (9)$$

with q_k the populations of atom k in the molecule, containing $N + 1$, N, or $N - 1$ electrons. The atomic charges can be obtained by a ChelpG population analysis[22] using a B3LYP/6-

31G* level of calculation in Gaussian 98. f_k^+ is the reactivity index for a nucleophilic attack and f_k^- for an electrophilic attack.

Because the local softness, $s(r)$, is related to the Fukui function through $s(r) = S\,f(r)$, the condensed local softness is related to the condensed Fukui function by[23]

$$s_k^i = f_k^i S \qquad i = + \text{ or } - \tag{10}$$

Both f_k and s_k describe local properties of the molecules thus allowing the possibility to discriminate between the reactivity of distinct atoms in a molecule. s_k is used in the local HSAB principle[24] that states that the original HSAB principle of Pearson[25] is still valid at the atomic level: soft atoms react preferentially with other soft atoms. To complete the analogy between local and global HSAB principle, the local hardness is required.

However, the definition of the local hardness is ambiguous. Berkowitz and Parr[26] showed that there exists a reciprocity relation between local hardness and local softness similar to the way global softness is the inverse of the global hardness. On the other hand, it can be proven that, for some choices, $\eta(r) = \eta$, a constant through space.[27]

By using the Thomas−Fermi−Dirac (TFD) approach to DFT, Berkowitz et al.[28] have put the local hardness in relation with the electrostatic potential

$$\eta_D^{TFD}(\mathbf{r}) \cong \frac{-V_{el}(\mathbf{r})}{2N} \tag{11}$$

where V_{el} represents the classical electrostatic potential due to the entire electron density. This relation can be used to evaluate approximate values of the local hardness.[29]

Because the definition of local hardness is ambiguous, the same is true for any condensed version of the local hardness. Despite this reality, we are interested in using a quantity for describing the hard−hard or charge controlled interactions as a counterpart of the condensed local softness describing the soft−soft or orbital controlled interactions, as recently stressed by Chattaraj.[30] When looking back at the original definition of hard and soft acids and bases, a hard acid has an acceptor atom with high positive charge. Therefore, the atomic charge is used here as a measure for the local hardness as they both quantify essentially the reactivity in charge controlled reactions or reaction steps. In this work, ChelpG charges, which are derived from the electrostatic potential,[22] are used as an approximation for the condensed local hardness

$$\eta_k \approx |q_k| \tag{12}$$

Obviously, the actual values q_k are dependent on the method used, however, trends obtained with the method and basis set used in this work can be expected to remain unaltered whatever the method or basis set.

In the framework of the local HSAB principle, softness matching is investigated through calculation of the difference in atomic softness between two atoms. By analogy, we also investigated hardness matching through calculation of the difference in atomic hardness. In the discussion of the results, not only the hardness matching is investigated, but also, the electrostatic interaction energy between two atoms is calculated.[30] This is done to emphasize that the interactions under investigation are charge controlled.

3. Results

3.1. Reaction Path for Ethylation of Benzene. The first reaction, the ethylation of benzene with ethene to form ethylbenzene, is shown in Figure 2. Benzene and ethene coadsorb at the Brønsted acid site (**eR**). The acid proton of the zeolite is in interaction with ethene, which is adsorbed as a π complex. After attack of the acid proton on ethene a positively charged carbenium ion is formed, which performs an electrophilic aromatic substitution on benzene. At the transition structure (**eTS**), the proton is already attached to a carbon of ethene, but the other carbon of ethene is not yet bonded with benzene. After the transition structure, the bond between ethyl and benzene will be formed and a proton of benzene will be given back to the zeolite to restore the electrical neutrality (**eP**).

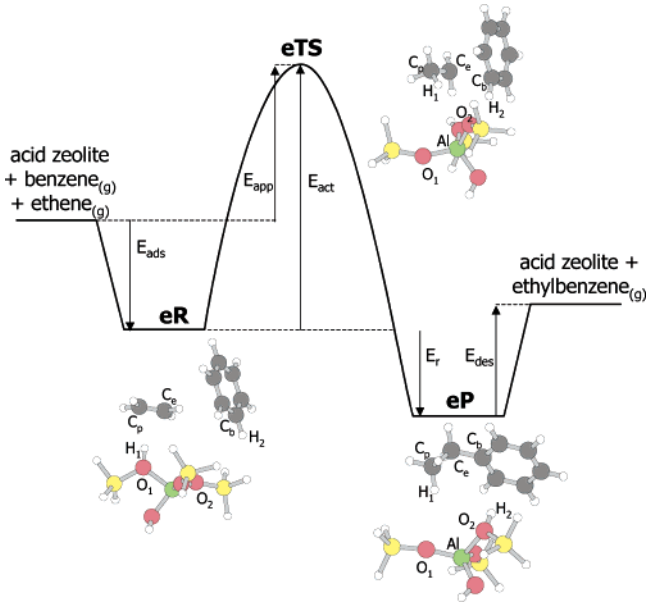

Figure 2. Reaction diagram for the ethylation of benzene to ethylbenzene.

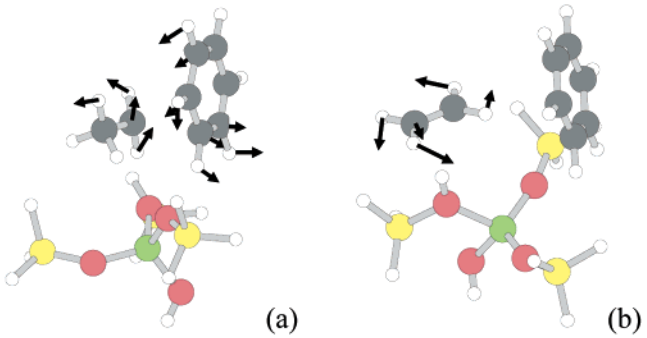

Figure 3. (a) Imaginary frequency at the transition structure, representing the reaction mode; (b) extra imaginary frequency for the adsorbed reactants corresponding to an internal rotational mode.

No stable charged intermediates were found during the reaction. The first structure that was optimized was the transition structure. This transition structure has one imaginary frequency representing the reaction coordinate (see Figure 3a). Deforming this structure a little in the direction of reactants and products respectively and optimizing until a minimum was found led to **eR** and **eP** as shown in Figure 2. More detailed information about the geometry and energy changes during reaction can be found in Table 1.

At the beginning of the reaction, the acid proton (H_1) is attached to one of the bridging oxygen atoms (O_1). The distance between this bridging oxygen and aluminum ($d(AlO_1)$) is longer than the other AlO distances. Ethene is adsorbed on this acid site ($d(H_1C_p) = 2.275$ Å) and there is a weaker interaction between benzene and both the active site of the zeolite and

TABLE 1: Geometrical and Energetical Characteristics for the Ethylation of Benzene[a]

	eR	eTS	eP
AlO_1	1.906	1.758	1.722
O_1H_1	0.985	3.690	2.853
H_1C_p	2.275	1.094	1.095
C_pC_e	1.338	1.495	1.540
C_eC_b	3.986	2.123	1.514
C_bH_2	1.086	1.092	2.729
H_2O_2	3.907	2.020	0.982
O_2Al	1.719	1.791	1.911
$C_pHH'C_e$	0.674	26.18	40.55
ν	−15.86	−199.83	
E_{ads}	−30.52		
E_{act}		131.92	
E_{app}		101.40	
E_r			−97.81
E_{des}			26.79

[a] Distances are in Å, angles are in degrees, energies are in kJ mol^{-1}, and the imaginary frequencies (ν) are in cm^{-1}. Full structure of eR, eTS, and eP can be found in the Supporting Information (Tables 1S−3S).

ethene ($d(H_2O_2)$ = 3.907 Å and $d(C_eC_b)$ = 3.986 Å). When the two molecules coadsorb at the acid site, 30.52 kJ mol^{-1} is set free (E_{ads}, see Figure 2).

The structure with the coadsorbed reactants, **eR**, was optimized with one imaginary frequency. This imaginary frequency corresponds to a rotation of ethene around the bridging hydroxyl group (see Figure 3b) and is very small (ν = −15.86 cm^{-1}). Several attempts to re-optimize the structure in order to eliminate this frequency were not successful. However, because the frequency is very small, it is believed that elimination would not alter the geometrical and energetical features of **eR** dramatically.

At the transition structure, the acid proton is already attached to one of the carbon atoms of ethene ($d(H_1C_p)$ = 1.094 Å). As a consequence, the AlO_1 distance is almost equal to the other AlO distances, the bond between the two carbon atoms loses its double bond character ($d(C_pC_e)$ = 1.495 Å), and the ethyl fragment is no longer planar ($C_pHH'C_e$-dihedral angle = 26.18°). The bond between the second carbon atom of ethene and one of the carbon atoms of benzene is not yet formed ($d(C_eC_b)$ = 2.123 Å). The activation energy for this reaction is 131.92 kJ mol^{-1}.

The reaction ends when the bond between the ethyl fragment and benzene is formed ($d(C_eC_b)$ = 1.514 Å) and benzene expels a proton, which bonds with a bridging oxygen atom of the cluster ($d(C_bH_2)$ = 2.729 Å and $d(H_2O_2)$ = 0.982 Å). Ethylbenzene is now adsorbed on an acid site of the zeolite cluster, and 26.79 kJ mol^{-1} of energy is necessary for desorption (E_{des}, see Figure 2).

3.2. Reaction Path for Isopropylation of Benzene. The isoproylation of benzene with propene is similar with the ethylation of benzene. The energy diagram is shown in Figure 4, with the adsorbed reactants (**iR**), transition structure (**iTS**), and adsorbed products (**iP**). Again starting from the transition structure and going downhill in the two different directions of the reaction path, **iR** and **iP** were obtained, respectively. A closer look at the reaction mechanism can be found in Table 2.

In going from the adsorbed reactants, **iR**, to the transition structure, **iTS**, the acid proton of the cluster, H_1, leaves the bridging oxygen of the cluster, O_1, and attaches to one of the carbon atoms of propene, C_p. As can be seen in Table 2, the O_1H_1 distance changes from 0.989 to 2.804 Å and the H_1C_p distance from 2.167 to 1.102 Å. As a consequence, the AlO_1 and C_pC_e distances change as well. There is not yet a bond formed between the propyl fragment and a carbon atom of benzene ($d(C_eC_b)$ = 2.283 Å), but the propyl fragment is moving toward benzene as the imaginary frequency of the transition structure corresponds to this movement (see Figure 5a). The energy difference between **iR** and **iTS** is 124.10 kJ mol^{-1}.

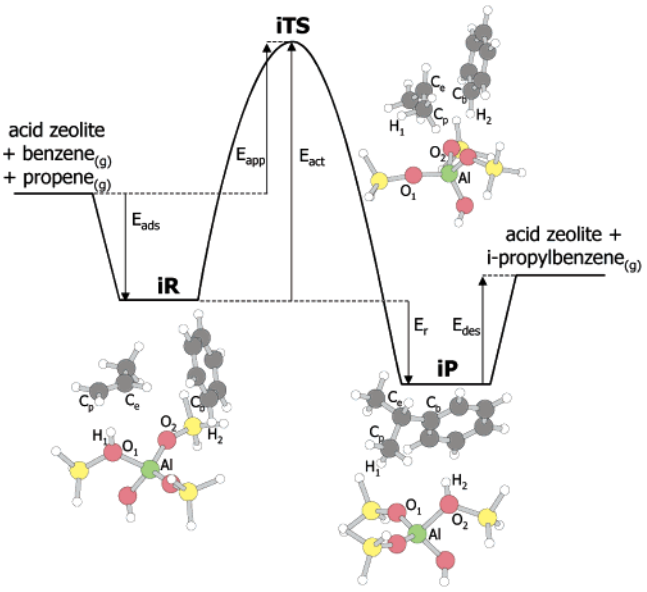

Figure 4. Reaction diagram for the isopropylation of benzene to cumene.

TABLE 2: Geometrical and Energetical Characteristics for the Isopropylation of Benzene

	iR	iTS	iP
AlO_1	1.902	1.760	1.719
O_1H_1	0.989	2.804	3.593
H_1C_p	2.167	1.102	1.096
C_pC_e	1.342	1.481	1.540
C_eC_b	4.067	2.283	1.523
C_bH_2	1.087	1.089	2.737
H_2O_2	4.129	2.337	0.983
O_2Al	1.720	1.791	1.920
C_eHCC_p	−0.01	16.13	38.63
ν		−114.00	−8.50
E_{ads}	−34.54		
E_{act}		124.10	
E_{app}		89.57	
E_r			−76.18
E_{des}			25.96

[a] Distances are in Å, angles are in degrees, energies are in kJ mol^{-1}, and the imaginary frequencies (ν) are in cm^{-1}. Full structure of iR, iTS, and iP can be found in the Supporting Information (Tables 4S−6S).

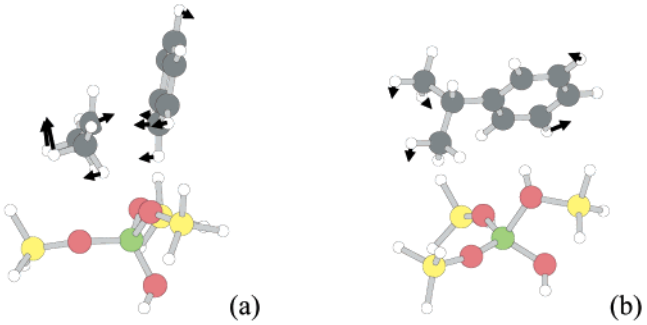

Figure 5. (a) Imaginary frequency at the transition structure, representing the reaction mode; (b) extra imaginary frequency for the adsorbed reactants corresponding to an internal rotational mode.

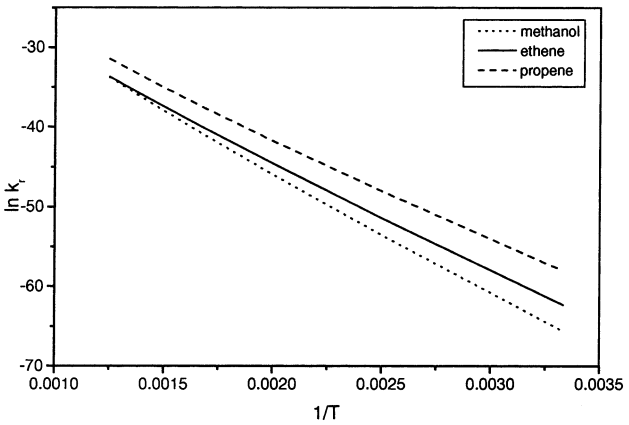

Figure 6. Arrhenius plots for the methylation, ethylation and isopropylation reaction of benzene with methanol, ethene, and propene, respectively.

TABLE 3: Summary of the Kinetic Analysis for the Methylation, Ethylation, and Isopropylation Reaction of Benzene, with Reaction Rate Constants at 400 K (k_r) in m^6 s^{-1} mol^{-2}, Arrhenius Activation Energies (E_{Arr}) in kJ mol^{-1}, the Preexponential Factors (A) in m^6 s^{-1} mol^{-2}, the Entropies of Activation (ΔS_{act}) in kJ mol^{-1} K^{-1}, and the Gibbs Free Energies of Activation (ΔG_{act}) in kJ mol^{-1}

	k_r (400 K)	E_{Arr}	A	ΔS_{act}	ΔG_{act}
ethylation	4.797×10^{-23}	114.22	4.99×10^{-7}	−0.315	233.52
isopropylation	1.984×10^{-21}	105.99	1.28×10^{-7}	−0.307	222.16
methylation	5.604×10^{-24}	127.12	3.03×10^{-7}	−0.300	240.42

After the transition structure, the bond between C_p and C_b is formed ($d(C_pC_b) = 1.523$ Å) and the newly formed cumene donates a proton, H_2, to the zeolite cluster. The C_bH_2 distance changes from 1.089 to 2.737 Å and the H_2O_2 distance from 2.337 to 0.983 Å.

Unfortunately, **iP** has one small imaginary frequency ($\nu = -8.50$ cm^{-1}). As can be seen in Figure 5b, this imaginary frequency corresponds to a movement of cumene above the zeolite cluster. Because the frequency is very small, it is believed that elimination would not alter the geometrical and energetic features of **iP** dramatically.

3.3. Rate Constants for the Ethylation and Isopropylation of Benzene. The rate constants for the ethylation and isopropylation reaction of benzene with ethene and propene are calculated in the temperature range from 300 to 800 K, using eq 1. The results can be seen in Figure 6 and Table 3. For comparison, the results for the methylation of benzene with methanol are also given.[10b] For all temperatures, the rate constants for the formation of cumene are the highest, followed by the ones for the formation of ethylbenzene and toluene. At higher temperature the difference between these three reactions becomes smaller, and the intercepts of the Arrhenius plots with the Y axis are almost equal. Consequently, the values of the pre-exponential factors, A, for the three reactions are close together, but the Arrhenius activation energy follows the order isopropylation < ethylation < methylation.

The activation entropy, ΔS_{act}, which is calculated from the pre-exponential factor, A, with eq 3, has similar values for the three reactions. ΔS_{act} has a negative sign because there is a loss in rotational and translational degrees of freedom in going from reactants to transition structure. The Gibbs free energy of activation, $\Delta G_{act} = E_{Arr} - 2RT - T\Delta S_{act}$, follows the same trend as the Arrhenius activation energy.

Formation of cumene from propene and benzene is the fastest reaction; formation of toluene from methanol and benzene the slowest. The reaction rate of the ethylation of benzene to form ethylbenzene is between the two other reactions (see Figure 6). Experimental results on the ethylation and isopropylation of benzene also indicate that isopropylation is a faster reaction than ethylation.[2f−i] Corma et al.[2f] reported an activation energy of 77 kJ mol^{-1} for isopropylation of benzene with propene over a MCM-22 zeolite with Si/Al = 15. The activation energy obtained in this study is larger. The cluster approximation does not take into account all of the stabilization effects of the zeolite lattice and has a different Si/Al ratio compared to the zeolites used in experiments. Other experimental studies on the isopropylation of benzene with 2-propanol instead of propene yield activation energies varying between 41.2 and 135.6 kJ mol^{-1}, depending on the structure type and chemical composition of the zeolite.[2h−i]

TABLE 4: Global Reactivity Descriptors for the Ethylation and Isopropylation of Benzene[a]

	$\eta_{reactants}$	η_{TS}	$\eta_{products}$	$\Delta\eta_{act}$
	$\eta = (IE - EA)/2$			
ethylation	0.1781	0.1246	0.1759	0.0535
isopropylation	0.1765	0.1112	0.1777	0.0653
	$\eta = (E_{HOMO} - E_{LUMO})/2$			
ethylation	0.1152	0.0572	0.1178	0.0581
isopropylation	0.1194	0.0471	0.1169	0.0723

[a] η is calculated using two different approximations (eqs 5 and 6) and is in atomic units.

3.4. Global Density Functional Based Reactivity Descriptors. The absolute hardness, η, of all of the optimized structures has been calculated in the finite difference approach (eq 5) and from the HOMO−LUMO gap (eq 6). The results are given in Table 4. The hardness of the transition structures, η_{TS}, is smaller than the hardness of the adsorption complexes of reactants and products ($\eta_{reactants}$, $\eta_{products}$). This is a manifestation of the maximum hardness principle: more stable structures or low energy structures are harder than less stable structures with a higher energy.[25]

The activation hardness, $\Delta\eta_{act} = \eta_{reactants} - \eta_{TS}$,[31] is also given in Table 4. Unlike for the methylation of toluene in ortho, meta, or para,[10b] no correlation between $\Delta\eta_{act}$ and the activation energy exists for the ethylation and isopropylation of benzene. Apparently, $\Delta\eta_{act}$ is only well suited to explain selectivity in reactions for which the starting points (adsorbed reactants in the case of zeolite catalyzed reactions) are similar[10b] and less suited to explain reactivity sequences for reactions with different reactant molecules.

3.5. Local Density Functional Based Reactivity Descriptors. The local HSAB indices are calculated for the adsorption complexes of reactants, because we want to be able to make predictions about the reactivity of the different systems without having to optimize transition structures. The most important atoms in the reactions are those that are involved in the bond breaking and bond making processes. For the calculation of the local reactivity descriptors, we therefore focused on (1) the acid proton of the cluster, (2) the carbon atom of ethene or propene that is protonated by the acid proton (C_p), (3) the electrophilic carbon atom of ethene or propene that bonds with benzene (C_e), and (4) the aromatic carbon atom of benzene that is attacked by the electrophilic carbon (C_b). The Fukui functions of these atoms are calculated with eqs 8 and 9 and are given in Table 5. f^+ is calculated for the atoms with an electrophilic behavior and f^- for nucleophilic atoms.

These Fukui functions are used for the calculation of the local softness (eq 10). The local hardness is approximated as the atomic charge obtained by a ChelpG-method (eq 11). Both local

TABLE 5: Atomic Fukui Functions for the Adsorbed Reactants before the Ethylation and Isopropylation of Benzene (in Atomic Units)

	f_H^+	f_{Cp}^-	f_{Ce}^+	f_{Cb}^-
ethylation	0.0486	0.0390	0.1673	−0.0555
isopropylation	0.0729	0.0624	0.1162	0.0227

TABLE 6: Local Reactivity Indices for the Ethylation and Isopropylation of Benzene[a]

	Δs_{HCp}	$\Delta\eta_{HCp}$	η_{Cp}	η_H	ΔE_{HCp}	$\Pi\eta_{HCp}$
ethylation	0.0269	0.1573	0.1737	0.3310	−0.0253	0.0575
isopropylation	0.0296	0.0140	0.3566	0.3426	−0.0564	0.1222
methylation with methanol[b]	0.1182	0.1957	0.5978	0.4021	−0.0911	0.2404

	Δs_{CeCb}	$\Delta\eta_{CeCb}$	η_{Cb}	η_{Ce}	ΔE_{CeCb}	$\Pi\eta_{CeCb}$
ethylation	0.4697[c]	0.1488	0.0862	0.2350	−0.0051	0.0203
isopropylation	0.2651	0.1087	0.1231	0.0144	−0.0017	0.0018
methylation with methanol	0.0777	0.1230	0.0259	0.1489	−0.0010	0.0039
with methoxide		0.0368	0.0672	0.1040	−0.0017	0.0070

[a] For comparison the local reactivity indices for the methylation of benzene with methanol (or methoxide) are also given. [b] Values calculated for oxygen atom of methanol instead of protonated carbon atom of alkene [c] Because f_{Cb}^- has a negative value, it has been set to zero for further calculations

softness and local hardness are used in the local HSAB principle. For orbital controlled reactions, the difference in softness (Δs_{AB}) of the two interacting atoms *A* and *B* should be as small as possible to promote the reaction. By analogy, one could propose that for charge-controlled reactions the difference in hardness ($\Delta\eta_{AB}$) of the two interacting atoms *A* and *B* should be as small as possible.[10b] Furthermore, we derived some other reactivity indices for charge controlled reactions: (1) η_B or the local hardness of the nucleophilic atom *B*; (2) ΔE_{AB} or the electrostatic interaction energy between the electrophilic atom *A* and the nucleophilic atom *B*, $\Delta E_{AB} = (q_A\, q_B)/R_{AB}$, with q_A and q_B the atomic charge on atoms *A* and *B*, R_{AB} is the distance between atom *A* and atom *B*; (3) $\Pi\eta_{AB}$ or the product of η_A and η_B. The larger these three quantities are, the more favored the reaction is.

The reaction starts with the protonation of a carbon atom, C_p of the alkene. To check the local HSAB principle for those two atoms (H and C_p), Δs_{HCp} and $\Delta\eta_{HCp}$ were calculated (see Table 6). The smaller these quantities are, the more favored the reaction is. Because isopropylation is easier than ethylation, Δs_{HCp} and/or $\Delta\eta_{HCp}$ for isopropylation must be smaller than for ethylation. The difference in local softness, Δs_{HCp}, does not give the right sequence (see Table 6), but the difference in local hardness, $\Delta\eta_{HCp}$, does yield a sequence in agreement with experimental observations. Apparently the formation of the new HC_p bond is a charge controlled reaction step. This is a logical assumption because a proton is known to be a hard reactant. To check this assumption, other reactivity indices for charge controlled reaction steps, η_{Cp}, ΔE_{HCp}, and $\Pi\eta_{HCp}$ were also calculated. These quantities must be as large as possible and all three yield the same reactivity sequence: isopropylation is more favored than ethylation.

The HC_p bond is not the only new bond formed in the reaction. The electrophilic carbon of the alkyl fragment (C_e) bonds with an aromatic carbon of benzene (C_b), and therefore, Δs_{CeCb} and $\Delta\eta_{CeCb}$ were also calculated (Table 6). Both indices, which must be as small as possible to favor a reaction, indicate that isopropylation is easier than ethylation and are in agreement with experimental observations. Therefore, it is not possible to conclude whether this step in the reaction is dominated by soft−soft interactions (orbital controlled, small Δs_{CeCb}) or hard−hard interactions (charge controlled, small $\Delta\eta_{CeCb}$). Because a charged alkyl fragment is a hard reactant, we would expect the reaction to be charge controlled, and for charge controlled reactions, η_{Cb}, ΔE_{CeCb}, and $\Pi\eta_{CeCb}$ should also be useful. These quantities must be as large as possible for charge controlled reactions. However, only η_{Cb} exhibits the right sequence, i.e., η_{Cb} for isopropylation is larger than η_{Cb} for ethylation.

For comparison, the reactivity indices for methylation of benzene with methanol are also given in Table 6.[10b] Methylation of benzene with methanol starts with methanol adsorbed by a strong H bond on the Brønsted acid site, whereas alkylation of benzene with an alkene starts with the alkene adsorbed on the Brønsted acid site through a weaker acid proton−π-cloud interaction. When the type of interaction changes, other reactivity descriptors will be important. In what follows, we will investigate whether it is possible to use the few reactivity descriptors, defined before, for comparing all of these different reactions.

When the reaction proceeds in the direct mechanism, the acid proton of the cluster will protonate the oxygen atom of methanol (O_m), and Δs_{HOm}, $\Delta\eta_{HOm}$, η_{Om}, ΔE_{HOm}, and $\Pi\eta_{HOm}$ were calculated here instead of the indices using C_p. The indices describing the interaction between the electrophilic carbon atom and the carbon atom of benzene were calculated for both the direct mechanism and the consecutive mechanism with intermediate formation of a methoxy species. These reactivity indices do not fit in the reactivity sequences as they are obtained for ethylation and isopropylation.

3.6. Discussion. The reactivity indices which describe the hard−hard interaction between the acid proton and the carbon atom of the alkene that is protonated (C_p), namely $\Delta\eta_{HCp}$, η_{Cp}, ΔE_{HCp}, and $\Pi\eta_{HCp}$ all indicate that isopropylation is favored over ethylation, in agreement with experimental data available. The picture emerging from the reactivity indices calculated for the C_eC_b interaction is not as clear as that from the reactivity indices calculated for the HC_p interaction. The reactivity sequence for alkylation of benzene by an alkene is determined early in the reaction, when the alkene is protonated and not when the C_eC_b bond is formed. This can also be the reason $\Delta\eta_{act}$ does not correlate with the activation energy and the experimental observations.

Reactivity indices can only be used for reactions which are similar, e.g., comparing reactivity of different alkenes for the alkylation of benzene or comparing selectivity for methylation of benzene or toluene with methanol. For the reactions that were studied here, three distinct reaction mechanisms exist: (1) The alkylation of benzene with an alkene starts with protonation of the alkene and the positively charged alkyl attacks the benzene. (2) Methylation with methanol in the direct mechanism also starts with protonation of methanol, but then CH_3^+ is separated from a H_2O molecule followed by the attack of the positively charged methyl group on the aromatic compound. (3) When first a methoxide is formed for methylation of benzene, the protonation step no longer occurs.

Changes in reaction mechanism, caused by other interaction types between the reactant and the Brønsted acid site of zeolites before reaction, are responsible for making the reactivity indices only useful in limited areas. When the type of interaction changes, other reactivity descriptors will be significant.

4. Alkoxy Species

4.1. Introduction. The traditional explanation for the mechanism of alkylation reactions over acid zeolites is based on

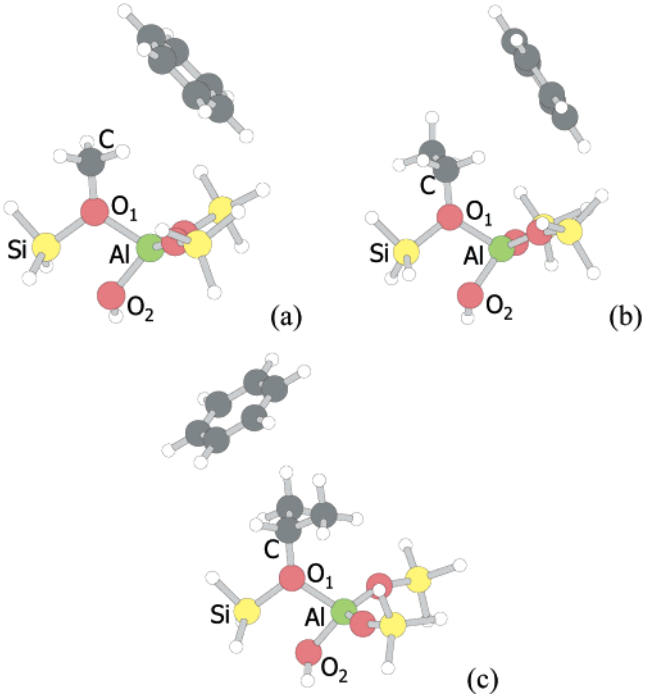

Figure 7. Geometry of (a) methoxide, (b) ethoxide, and (c) propoxide.

carbenium ion intermediates. However, experimentally, only very stable carbocations are observed in zeolites,[32] and the existence of free carbenium ions for nonbranched light alkenes is questioned. An alternative explanation for the reaction mechanism assumes a concerted mechanism. Because the transition structures in this mechanism have a cationic character, they obey all rules of carbenium ion chemistry. Alkoxy species, formed when protonated alkenes covalently bond with one of the bridging oxygens, are often suggested to be intermediates in these concerted reactions. In contrast to carbocations, there exists experimental evidence for the existence of alkoxy species.[33] Theoretical calculations indicate that alkoxy species are local minima or stable structures and carbocations are transition structures.[34]

The reaction mechanism for the ethylation and isopropylation of benzene as calculated in this work proceeds in one step, without formation of alkoxy species. Therefore, some additional calculations were done to verify whether the reaction is also possible with intermediate alkoxy formation.

4.2. Results and Discussion. Alkoxy species are more stable than the corresponding π complexes. Their structure is given in Figure 7 and Table 7. Going from methoxide over ethoxide to isopropoxide, the charge on the alkyl group, obtained by a ChelpG population analysis, increases or the alkyl group gets a more carbenium ion-like character. The bond length between the oxygen atom of the cluster and the carbon atom of the alkyl group increases together with this carbenium ion character, in agreement with experiment.[35] In the case of a π complex, the charge transfer between the zeolite cluster and the adsorbed alkene is very small (less than 0.07e).

However, the cluster is deformed when alkoxy species are formed: the SiO_1Al angle becomes smaller as is the distance between the terminating hydroxyl of the cluster and the silicon atom ($d(SiO_2)$). It is difficult to predict whether such a deformation is possible in real zeolite structures, and therefore, it cannot be guaranteed that alkoxy species in real zeolites are still more stable than the corresponding π complexes. Furthermore, when, starting from the transition structure geometry, the structure of the nearest minimum in the direction of the reactants is optimized, no alkoxy species are encountered. Therefore, it is believed that these structures do not occur in the reaction. This is in agreement with a DFT study of Milas and Nascimento about the dehydrogenation of isobutane over zeolites.[36] They calculated the complete reaction path (IRC) and found no evidence for alkoxy species.

When only the energy of the local minima on the PES are considered, one could conclude that alkoxy species are important in the reaction mechanism, but after a more detailed study on how the different minima and transition structures are connected with each other, it appears that alkoxy species are not important structures in the reaction. Experimentally, similar results were obtained by Ivanova and Corma[37] and by Mirth and Lercher[38] for the methylation with methanol. Although methoxy species are formed during reactions, they appear not to be reactive and reaction is preceded by coadsorption of methanol and benzene or toluene.

TABLE 7: Comparison between Three Different Alkoxy Species: Methoxide, Ethoxide, and Isopropoxide, with Al−O and O−C distances in Å, SiOAl and OAlO angles in Degrees, the Charge on the Alkyl Group in Electrons, the Energy Difference with the Transition Structure of the Studied Reaction (ΔE) in kJ mol^{-1}, and the Hardness (η) Calculated with eq 5 (in Atomic Units)[a]

		ethoxide		isopropoxide	
	methoxide	alkoxy	π-complex	alkoxy	π complex
AlO_1	1.892	1.898	1.906	1.892	1.902
O_1C	1.450	1.466	4.240	1.480	3.980
SiO_1Al	110.41	111.50	114.99	108.97	115.83
SiO_2	2.3181	2.4002	2.5334	2.2752	2.5963
q_{alkyl}	0.1666	0.2446		0.2918	
q_{alkene}			0.0667		0.0548
q_H			0.3310		0.3428
ΔE	186.40	190.75	131.92	173.89	124.10
η	0.1823	0.1806	0.1781	0.1800	0.1765

[a] For comparison, these quantities are also given for the corresponding π complexes.

5. Conclusion

The reaction mechanism for the ethylation and isopropylation of benzene with ethene and propene was investigated. The reactions follow a concerted pathway with a cyclic transition structure. However, not all of the bonds are broken or formed to the same extent in the transition structure: The bond between the acid proton and the carbon atom of the alkene is already formed in the transition structure; the bond between the electrophilic carbon atom of the alkene and the carbon atom of benzene is in the process of being formed in the transition structure; the bond breaking between the carbon atom and the proton of benzene occurs after the transition structure. This asynchronous pathway does not result in the formation of stable charged intermediates. It has also been shown that formation of alkoxy species is not required to initiate the reaction but that adsorbed alkenes are responsible for alkylation of benzene.

Kinetic analysis showed that isopropylation of benzene with propene is faster than ethylation with ethene: the isopropylation reaction has a larger rate constant, k_r, a smaller Arrhenius activation energy, E_{Arr}, and a smaller Gibbs free energy of activation, ΔG_{act}. The same reactivity sequence was obtained by a sensitivity analysis: for the isopropylation reaction $\Delta\eta_{HCp}$ is smaller than for the ethylation reaction and η_{Cp}, ΔE_{HCp}, and $\Pi\eta_{HCp}$ are larger. The bond between the acid proton and the carbon atom of the alkene is the first bond to be formed during reaction, and its formation is initiated by charge-controlled interactions in the adsorption complex of reactants. The reactiv-

ity difference between ethene and propene is determined by these interactions.

Acknowledgment. This work has been performed with support from the G.O.A. (Geconcerteerde Onderzoeksactie Vlaanderen). The authors acknowledge the Free University of Brussels (V.U.B.) for a generous computer grant. A.M.V. thanks the I.W.T and F.W.O. for financial support, and P.G. thanks the Fund for Scientific Research-Flanders (F.W.O) for continuous support of his group.

Supporting Information Available: Atomic coordinates for the optimized structures of the adsorbed reactants, transtition states and adsorbed products are given for the ethylation and isopropylation reaction of benzene. This material is available free of charge via the Internet at http://pubs.acs.org.

References and Notes

(1) Weisselmel, K.; Arpe, H. *Industrial Organic Chemistry*; Verlag Chemie: New York, 1994; p 333.

(2) (a) Keading, W. W.; Young, B. L.; Chu, C. C. *J. Catal*. **1984**, *89*, 267. (b) Keading, W. W. *J. Catal*. **1985**, *95*, 512. (c) Cejka, J.; Wichterlova, B.; Bednarova, S. *Appl. Catal*. **1991**, *79*, 215. (d) Wichterlova, B.; Cejka, J. *J. Catal*. **1994**, *146*, 523. (e) Ivanova, I. I.; Brunel, D.; Nagy, J. B.; Derouane, E. G. *J. Mol. Catal. A* **1995**, *95*, 243. (f) Corma, A.; Martinez-Soria, V.; Schnoeveld, E. *J. Catal*. **2000**, *192*, 163. (g) Du, Y.; Wang, H.; Chen, S. *J. Mol. Catal. A* **2002**, *179*, 253. (h) Sridevi, U.; Bokade, V. V.; Satyanarayana, C. V. V.; Rao, B. S.; Pradhan, N. C.; Rao, B. K. B. *J. Mol. Catal. A* **2002**, *181*, 257. (i) Sridevi, U.; Rao, B. K. B.; Pradhan, N. C.; Tambe, S. S.; Satyanarayana, C. V.; Rao, B. S. *Ind. Eng. Chem. Res.* **2001**, *40*, 3133.

(3) (a) Frank, B.; Dahlke, K.; Emig, G.; Aust, E.; Broucek, R.; Nywlt, M. *Microporous Mater*. **1993**, *1*, 43. (b) Snurr, R. Q.; Bell, A. T.; Theodorou, D. N. *J. Phys. Chem*. **1993**, *97*, 13742. (c) Horsley, J. A.; Fellmann, J. D.; Derouane, E. G.; Freeman, C. M. *J. Catal*. **1994**, *147*, 231. (d) Deka, R. C.; Vetrivel, R. *Chem. Commun*. **1996**, 3297.

(4) (a) Sauer, J. *Chem. Rev*. **1989**, *89*, 199. (b) Kramer, G. J.; van Santen, R. A.; Emeïs, C. A.; Nowak, A. K. *Nature*. **1993**, *363*, 529. (c) van Santen, R. A.; Kramer, G. J. *Chem. Rev*. **1995**, *95*, 637. (d) Blaszkowski, S. R.; van Santen, R. A. *J. Am. Chem. Soc*. **1997**, *119*, 5020. (e) Sandré, E.; Payne, M. C.; Gale, J. D. *Chem. Commun*. **1998**, 2445. (f) Stich, I.; Gale, J. D.; Terakura, K.; Payne, M. C. *J. Am. Chem. Soc*. **1999**, *121*, 3292. (g) Rozanska, X.; van Santen, R. A.; Hutschka, F.; Hafner, J. *J. Am. Chem. Soc*. **2001**, *123*, 7655.

(5) Sponer, J. J.; Sponer, J.; Cejka, J.; Wichterlova, B. *J. Phys. Chem. B* **1998**, *102*, 7169.

(6) Deka, R. C.; Pal, S.; Goursot, A.; Vetrivel, R. *Catal. Today* **1999**, *49*, 221.

(7) Song, C.; Ma, X.; Schmitz, A. D.; Schobert, H. H. *Appl. Catal. A* **1999**, *182*, 175.

(8) Clark, L. A.; Snurr, R. Q. *Stud. Surf. Sci. Catal*. **2001**, *135*

(9) (a) Vos, A. M.; Rozanska, S.; Schoonheydt, R. A.; van Santen, R. A.; Hutschka, F.; Hafner, J. *J. Am. Chem. Soc.* **2001**, *123*, 2799. (b) Vollmer, J. M.; Truong, T. N. J. *Phys. Chem. B* **2000**, *104*, 6308. (c) Sierka, M.; Sauer, J. *J. Phys. Chem. B* **2001**, *105*, 1603. (d) Rozanska, X.; van Santen, R. A.; Hutschka, F.; Hafner, J. *J. Am. Chem. Soc.* **2001**, *123*, 7655.

(10) (a) Vos, A. M.; De Proft, F.; Schoonheydt, R. A.; Geerlings, P. *Chem. Commun*. **2001**, 1108. (b) Vos, A. M.; Nulens, K. H. L.; De Proft, F.; Schoonheydt, R. A.; Geerlings, P. *J. Phys. Chem. B* **2002**, *106*, 2026.

(11) Brand, H. V.; Curtuss, L. A.; Iton, L. E. *J. Phys. Chem*. **1992**, *96*, 7725.

(12) Frisch, M. J.; Trucks, G. W.; Schlegel, H. B.; Scuseria, G. E.; Robb, M. A.; Cheeseman, J. R.; Zakrzewski, V. G.; Montgomery, J. A., Jr.; Stratmann, R. E.; Burant, J. C.; Dapprich, S.; Millam, J. M.; Daniels, A. D.; Kudin, K. N.; Strain, M. C.; Farkas, O.; Tomasi, J.; Barone, V.; Cossi, M.; Cammi, R.; Mennucci, B.; Pomelli, C.; Adamo, C.; Clifford, S.; Ochterski, J.; Petersson, G. A.; Ayala, P. Y.; Cui, Q.; Morokuma, K.; Malick, D. K.; Rabuck, A. D.; Raghavachari, K.; Foresman, J. B.; Cioslowski, J.; Ortiz, J. V.; Stefanov, B. B.; Liu, G.; Liashenko, A.; Piskorz, P.; Komaromi, I.; Gomperts, R.; Martin, R. L.; Fox, D. J.; Keith, T.; Al-Laham, M. A.; Peng, C. Y.; Nanayakkara, A.; Gonzalez, C.; Challacombe, M.; Gill, P. M. W.; Johnson, B. G.; Chen, W.; Wong, M. W.; Andres, J. L.; Head-Gordon, M.; Replogle, E. S.; Pople, J. A. *Gaussian 98*, revision A.7; Gaussian, Inc.: Pittsburgh, PA, 1998.

(13) (a) Becke, A. D. *J. Chem. Phys*. **1993**, *98*, 5648. (b) Lee, C.; Yang, W.; Parr, R. G. *Phys. Rev. B* **1988**, *37*, 785.

(14) (a) Zygmunt, S. A.; Mueller, R. M.; Curtiss, L. A.; Iton, L. E. *J. Mol. Struct. (THEOCHEM)* **1998**, *430*, 9. (b) Zygmunt, S. A.; Curtiss, L. A.; Zapol, P.; Iton, L. E. *J. Phys. Chem. A* **2000**, *104*, 1944.

(15) (a) Eyring, H. *J. Chem. Phys*. **1934**, *3*, 107. (b) Glasstone, S. *Physical Chemistry*; D. Van Nostrand Company, Inc: Toronto, 1946. (c) Robinson, P. J. *J. Chem. Educ*. **1978**, *55*, 509.

(16) Scott, A. P.; Radom, L. *J. Phys. Chem*. **1996**, *100*, 16502.

(17) (a) Parr, R. G.; Yang, W. *Density Functional Theory of Atoms and Molecules*; Oxford University Press: Oxford, 1989. (b) Parr, R. G.; Yang, W. *Annu. Rev. Phys. Chem*. **1995**, *46*, 701. (c) Geerlings, P.; De Proft, F.; Langenaeker, W. *Adv. Quantum Chem*. **1999**, *39*, 303. (d) Chermette, H. *J. Comput. Chem*. **1999**, *20*, 129. (e) De Proft, F.; Geerlings, P. *Chem. Rev*. **2001**, *101*, 1451. (f) Geerlings, P.; De Proft, F.; Langenaeker, W. *Chem. Rev.* submitted.

(18) Pearson, R. G.; Parr, R. G. *J. Am. Chem. Soc*. **1983**, *105*, 7512.

(19) Parr, R. G.; Yang, W. *J. Am. Chem. Soc*. **1984**, *106*, 4049.

(20) Fukui, K. Yonezawa, T.; Shingu, H. *J. Chem. Phys*. **1952**, *20*, 722.

(21) Yang, W.; Mortier, W. J. *J. Am. Chem. Soc*. **1986**, *108*, 5708.

(22) Breneman, C. M.; Wiberg, K. B. *J. Comput. Chem.* **1990**, *11*, 361.

(23) Yang, W.; Parr, R. G. *Proc. Nat. Acad. Sci. U.S.A.* **1985**, *82*, 6723.

(24) (a) Gazquez, J. L.; Mendez, F. *J. Phys. Chem*. **1994**, *98*, 4591. (b) Damoun, S.; Van de Woude, G.; Mendez, S.; Geerlings, P. *J. Phys. Chem. A* **1997**, *101*, 886. (c) Geerlings, P.; De Proft, F. *Int. J. Quantum Chem*. **2000**, *80*, 227.

(25) Pearson, R. G. *Hard and Soft Acids and Bases*; Dowen, Hutchinson and Ross: Stroudsberg, 1973.

(26) Berkowitz, M.; Parr, R. G. *J. Chem. Phys.* **1988**, *88*, 2554.

(27) Harbola, M. K.; Chattaraj, P. K.; Parr, R. G. *Isr. J. Chem*. **1991**, *31*, 395.

(28) Berkowitz, M.; Ghosh, S. K.; Parr, R. G. *J. Am. Chem. Soc*. **1985**, *107*, 6811.

(29) (a) Langenaeker, W.; De Proft, F.; Geerlings, P. *J. Phys. Chem*. **1995**, *99*, 6424. (b) Geerlings, P.; Langenaeker, W.; De Proft, F.; Baeten, A. Molecular Electrostatic Potentials vs DFT descriptors of reactivity. In *Molecular Electrostatic Potentials − Concepts and Applications (Theoretical and Computational Chemistry)*; 1996; Vol. 3, p 587.

(30) Chattaraj, P. K.; *J. Phys. Chem. A* **2001**, *105*, 511.

(31) Zhou, Z.; Parr, R. G. *J. Am. Chem. Soc*. **1990**, *112*, 5720.

(32) (a) Haw, J. F.; Richardson, B. R.; Oshiro, I. S.; Lazo, N. L.; Speed, J. A. *J. Am. Chem. Soc.* **1989**, *111*, 2052. (b) Tao, T.; Maciel, G. *J. Am. Chem. Soc*. **1995**, *117*, 12889. (c) Xu, T.; Barich, D. H.; Goguen, P. W.; Song, W.; Wang, Z.; Nicholas, J. B.; Haw, J. F. *J. Am. Chem. Soc*. **1998**, *120*, 4025.

(33) (a) Kubelkova, L.; Novakova, J.; Nedomova, K. *J. Catal*. **1990**, *124*, 441. (b) Bosacek, V. *J. Phys. Chem*. **1993**, *97*, 10732.

(34) Kazansky, V. B. *Acc. Chem. Res*. **1991**, *24*, 379.

(35) (a) Aronson, M. T.; Gorte, R. J.; Farneth, W. E. *J. Catal*. **1987**, *105*, 455. (b) Aronson, M. T.; Gorte, R. J.; Farneth, W. E.; White, D. *J. Am. Chem. Soc*. **1989**, *111*, 840. (c) Stepanov, A. G.; Maryasov, A. G.; Romannikov, V. N.; Zamaraev, K. I.; *Magn. Reson. Chem*. **1994**, *32*, 16.

(36) Milas, I.; Nascimento, M. A. C. *Chem. Phys. Lett*. **2001**, *338*, 67.

(37) Ivanova, I. I.; Corma, A. *J. Phys. Chem. B* **1997**, *101*, 547.

(38) (a) Mirth, G.; Lercher, J. A. *J. Phys. Chem*. **1991**, *95*, 3736. (b) Mirth, G.; Lercher, J. A. *J. Catal*. **1991**, *132*, 244.